Khazar Journal of Water and Environment
DOI: 10.68277/kjwe.2026.10

e-ISSN: 3150-0188
khazarjournal.com

KJWE

Urbanization-Induced Shifts in Hydrological Response of a Metropolitan Watershed

Farzaneh Tashtari [a], Arash Malekian*[b], Heidi Elisabeth Megerle [c], Sina Ebadi [d]

[a] *Department of Natural Resources Policy, Faculty of Natural Resources, University of Tehran, Karaj, Iran.*
[b] Faculty of Natural Resources, University of Tehran, Karaj, Iran
[c] *Chair of Applied Geography and Planning, Rottenburg University of Applied Forest Sciences, Rottenburg am Neckar, Germany*
[d] M.Sc. Student, Department of Spatial Information Systems, Faculty of Surveying, University of Tehran, Tehran, Iran

ARTICLE INFO
Research Article
Corresponding Author: Arash Malekian, E-mail: malekian@ut.ac.ir
Received: 24 August 2026 / Revised: 29 September 2026 / Accepted: 4 October 2026 / Online: 1 November 2026

Cite this article as
TASHTARI, F., MALEKIAN, A., MEGERLE, H.E. & EBADI, S. (2026). Urbanization-Induced Shifts in Hydrological Response of a Metropolitan Watershed. Khazar Journal of Water and Environment, 1, 221-241. DOI: 10.68277/kjwe.2026.10

ABSTRACT

Rapid urban expansion in semi-arid metropolitan areas alters hydrological response, yet the shift in the runoff initiation threshold—the minimum rainfall depth to generate surface runoff—remains poorly quantified. This study assesses this shift in District 22 of Tehran using Landsat-based land-use mapping, Random Forest classification in Google Earth Engine, and the SCS-CN model. The novelty lies in targeting the runoff initiation threshold as a primary variable, isolating land-cover effects under a constant design storm, and providing a replicable framework for data-scarce catchments. Impervious surfaces expanded from 38.2% to 64.7%, while pervious cover declined from 56.8% to 31.2%. The weighted Curve Number increased from 83.55 to 86.39, and potential maximum retention decreased from 50 mm to 40 mm, indicating reduced infiltration capacity. Consequently, the runoff initiation threshold dropped from 10 mm to 8 mm. Under a constant 100 mm design storm, direct runoff increased from 57.9 mm to 64.1 mm over the two decades. A sensitivity analysis on the Ia/S ratio (0.05–0.3) confirmed the robustness of these changes. The integration of remote sensing and hydrological modelling offers a practical tool for data-scarce regions. Due to only three time slices (2001, 2011, 2021), trends are reported descriptively without statistical significance claims. These findings demonstrate that urbanization has lowered the rainfall threshold for runoff, increasing flash flood risk. Low-impact development measures—permeable pavements, rain gardens, and infiltration trenches—are recommended for the western and central sectors of District 22. The proposed framework can support evidence-based stormwater management in rapidly growing cities with limited hydrological data

Keywords: Runoff initiation threshold, Urban hydrology, Landsat imagery, Random Forest

1. Introduction

Rapid urban expansion is widely recognized as a primary driver of hydrological transformation in metropolitan regions worldwide. The conversion of pervious surfaces—vegetated areas, open soils, and natural drainage paths—into impervious cover such as buildings, roads, and parking lots systematically alters the rainfall–runoff relationship. This alteration reduces infiltration capacity, shortens concentration time, increases the frequency and magnitude of surface runoff, and ultimately elevates flood risk in downstream areas (Jacobson, 2011; Shuster et al., 2005; Ahiablame et al., 2012). In semi-arid environments, where annual precipitation is low but rainfall events are often short and high-intensity, even moderate increases in imperviousness can generate disproportionately large runoff responses. Under such climatic conditions, the hydrologic system operates close to a threshold: small reductions in surface storage capacity can produce sharp increases in runoff generation (Ponce & Hawkins, 1996; Mishra & Singh, 2003).

Tehran, the largest metropolitan area in Iran, exemplifies this process. The city has experienced sustained and often unplanned urban growth over the past two decades, particularly in its western and northwestern districts. District 22 of Tehran Municipality—originally designed as a peri-urban extension with a mix of residential, recreational, and agricultural land uses—has undergone one of the fastest rates of physical development in the capital (Zarghamfard et al., 2023). Municipal reports and satellite observations indicate that extensive tracts of permeable soil, semi-natural vegetation, and dry farmland have been replaced by large-scale residential complexes, highways, commercial zones, and associated infrastructure. While the qualitative direction of change is well understood (i.e., more built-up area, less green space), quantitative assessments of how this land-use transition has modified the actual rainfall depth required to initiate surface runoff remain notably scarce. Most previous studies on Tehran's urban hydrology have focused on either total runoff volume estimation or flood hazard mapping, without explicitly examining the triggering condition of runoff itself (Behnam et al., 2013). For instance, Amiraslani (2021) applied the SCS-CN method to the Darabad basin in Tehran and reported that a rise in built-up land use substantially increased flood volume and peak discharge under specific return periods. However, their analysis concentrated on flood volume and peak discharge rather than on the minimum rainfall depth required to initiate runoff. Similarly, Behnam et al (2013) documented increasing runoff coefficients in Tehran's western suburbs but did not quantify the associated shift in the runoff initiation threshold. This represents a significant knowledge gap, particularly in semi-arid metropolitan areas where rainfall is limited but flash floods are recurrent and damaging.

In urban hydrology, the concept of the runoff initiation threshold—defined as the minimum rainfall depth necessary to overcome initial abstractions (including interception, depression storage, wetting of the surface, and initial infiltration) and generate measurable surface flow—provides a sensitive and process-oriented indicator of catchment response (USDA-NRCS, 1986; Hawkins et al., 2009). A lowering of this threshold implies that smaller, more frequent rainfall events become capable of producing runoff. This shift has direct practical consequences: urban drainage systems designed for larger, less frequent storms may become overwhelmed under previously innocuous rainfall conditions, leading to localized flooding, water quality

deterioration, and increased maintenance costs (Soulis & Valiantzas, 2012). Despite its practical importance, the runoff initiation threshold has received considerably less attention in urbanization-impact studies than total runoff volume, peak discharge, or flood extent mapping. This represents a significant knowledge gap, particularly in semi-arid metropolitan areas where rainfall is limited but flash floods are recurrent and damaging. Without explicitly quantifying how the threshold has changed over time, urban planners and water managers lack a crucial piece of information for designing adaptive stormwater infrastructure.

The Soil Conservation Service Curve Number (SCS-CN) method provides a well-established empirical framework for linking land cover, hydrologic soil group, and antecedent moisture conditions to direct runoff estimation (USDA-NRCS, 1986; Ponce & Hawkins, 1996). Within this framework, the initial abstraction I_a (conventionally taken as 0.2 of potential maximum retention S) directly represents the rainfall depth that must be exceeded before any runoff is generated. Therefore, by estimating S (and consequently I_a) from land-use/land-cover (LULC) and soil data, the SCS-CN method allows retrospective reconstruction of the runoff initiation threshold and its temporal evolution. When combined with multi-temporal remote sensing and machine learning classification, this approach can quantify how urban expansion has progressively lowered the threshold over decadal time scales. Recent advances in cloud-based platforms such as Google Earth Engine (Gorelick et al., 2017) and robust non-parametric classifiers like Random Forest (Breiman, 2001; Belgiu & Drăguț, 2016) have made it feasible to map LULC dynamics over extended periods with acceptable accuracy, even in data-scarce or rapidly changing urban settings. These technological developments open the possibility of conducting long-term, spatially explicit hydrological assessments without requiring extensive field instrumentation.

It is important, however, to acknowledge the methodological constraints of the SCS-CN approach when applied to long-term urbanizing catchments. The SCS-CN method was originally developed for event-based rainfall (USDA-NRCS, 1986; Ponce & Hawkins, 1996), and its application to annual precipitation totals can produce physically inconsistent results (Hawkins et al., 2009). Furthermore, the conventional assumption $I_a = 0.2S$ is known to perform poorly for highly impervious urban surfaces, where initial abstraction may be substantially lower (Hawkins et al., 2009; Soulis & Valiantzas, 2012). Alternative approaches such as SWMM, HEC-HMS, or physically based distributed models offer greater process representation but require extensive calibration data that are rarely available in data-scarce semi-arid catchments (Zakizadeh et al., 2022). This study therefore adopts a design-storm approach—applying a constant rainfall depth to all time slices—which isolates the effect of LULC change from interannual precipitation variability and avoids the physical inconsistency of applying event-based SCS-CN to annual totals. A sensitivity analysis on the I_a/S ratio is conducted to assess the robustness of the findings across a range of plausible λ values.

The knowledge gap that this study addresses can be stated as follows: while it is generally accepted that urbanization increases runoff volume, there is limited quantitative evidence on how urban expansion in a semi-arid metropolitan context has altered the minimum rainfall depth required to initiate surface runoff. Specifically, for District 22 of Tehran—a rapidly developing area with documented land-cover change—no previous study has systematically estimated the decadal change in the runoff initiation threshold using an

integrated remote sensing-hydrological modelling framework. Consequently, it remains unclear whether the threshold has remained stable, declined moderately, or dropped substantially, and what the magnitude of any such change implies for flood susceptibility under small to moderate rainfall events. This gap is not merely academic: in a semi-arid city like Tehran, where water scarcity coexists with flash flood risk, understanding the threshold shift is essential for designing proportional and cost-effective stormwater interventions.

The novelty of the present study lies in its explicit, quantitative, and time-explicit focus on the runoff initiation threshold as a primary response variable, rather than as a derived or secondary output. Unlike previous research that has primarily reported increases in Curve Number or runoff volume, this study directly translates LULC changes into changes in the rainfall depth required to start runoff. By applying a constant design-storm rainfall to three time slices (2001, 2011, and 2021), the analysis isolates the effect of land-cover change from interannual climatic variability, thereby distinguishing the anthropogenic signal of urbanization from climatic noise. The integration of Landsat-based LULC classification (Random Forest in Google Earth Engine), hydrologic soil group mapping (FAO-based groups C and D), and the SCS-CN model within a consistent GIS framework provides a replicable methodology that can be applied to other semi-arid urban catchments with similar data constraints. It should be emphasized, however, that the runoff initiation threshold in this study is not independently measured in the field but derived from the SCS-CN model; this limitation is explicitly acknowledged and discussed in the context of the study's findings.

Accordingly, the objective of this study is to assess the impact of urban expansion and associated LULC change on the surface runoff initiation threshold in the study area over the period 2001–2021. Specifically, the study seeks to: (i) quantify changes in impervious and pervious surface areas using multi-temporal Landsat imagery and Random Forest classification; (ii) estimate temporal variations in weighted Curve Number (CN), potential maximum retention (S), initial abstraction (I_a), and direct runoff (Q) using the SCS-CN model under a constant design-storm rainfall; (iii) determine the runoff initiation threshold (defined as I_a) for each time slice; (iv) describe the direction and relative magnitude of observed trends over the 20-year period, with explicit acknowledgement that formal statistical significance testing is not possible with three time slices; and (v) discuss the implications of any threshold reduction for urban flood risk and stormwater management in a semi-arid metropolitan context. The findings are expected to provide evidence-based support for low-impact development planning, green infrastructure placement, and flood risk reduction strategies in rapidly growing semi-arid cities, with District 22 serving as a representative case.

2. Material and Methods

2.1. Study Area

District 22 of Tehran Municipality, located in the western part of the Tehran metropolitan area (approximately 35°41′ to 35°48′ N and 51°08′ to 51°23′ E), was selected as the study area. The district covers roughly 85 km² and has experienced one of the fastest rates of urban expansion in the capital over the past two decades

(Zarghamfard et al., 2023). According to the Köppen–Geiger classification, the region has a cold semi-arid climate (BSk), with mean annual precipitation of approximately 239 mm based on 1991–2020 records from the Mehrabad synoptic station. Rainfall is concentrated between late autumn and early spring, and potential evapotranspiration exceeds precipitation for most of the year. Soils are predominantly alluvial deposits with low to moderate permeability. Based on FAO-derived soil data and local surveys, most of the study area falls into Hydrologic Soil Groups C and D according to USDA-NRCS (2009) criteria, which implies inherently high runoff potential under saturated conditions. The population of the district grew from approximately 150,000 in 2001 to over 400,000 in 2021, driving large-scale conversion of permeable land into residential complexes, commercial zones, and transport infrastructure.(Fig 1)

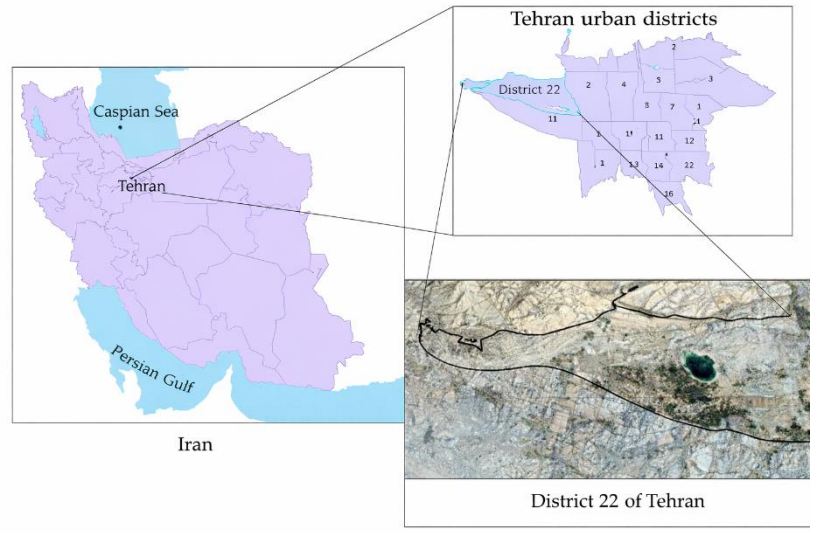


Figure 1. Study area: Tehran metropolitan

2.2. Satellite Data and Pre-processing

Multi-temporal Landsat imagery was used to map land-use and land-cover changes for three representative years: 2001, 2011, and 2021. The specific sensors were Landsat 7 ETM+ (2001), Landsat 5 TM (2011), and Landsat 8 OLI/TIRS (2021). These three epochs were selected to represent the major phases of urban development in District 22: pre-expansion, peak expansion, and post-expansion. The decadal interval is sufficient to capture the cumulative signal of urbanization on LULC, although it cannot resolve intra-decadal dynamics. The choice was also constrained by the availability of cloud-free summer imagery from the three sensors for path/row 165/35. This limitation is acknowledged in Section 4.4. All images corresponded to path and row 165/35, were acquired during the summer months (June to August) to minimize seasonal vegetation differences, and had less than 10% cloud cover. The imagery was accessed and processed using Google Earth Engine (Gorelick et al., 2017), which provides Collection 2 Level-2 surface reflectance products with built-in atmospheric correction. Pre-processing included cloud and cloud-shadow masking using the quality assessment band and spatial sub setting to the study area boundary. To enhance spectral separability among land-use and land-cover classes, two spectral indices were calculated for each image: NDVI and NDBI. The

use of only two indices was a deliberate choice to maintain consistency across the three sensors, because some indices require bands that are not equally available or comparable across Landsat 7, 5, and 8. This may limit discrimination of water bodies and sparse vegetation; therefore, per-class accuracy is reported to quantify classification uncertainty (Section 2.4). The Normalized Difference Vegetation Index (NDVI) was computed as:

$$NDVI = \frac{NIR-Red}{NIR+Red} \quad (1)$$

where NIR and Red are the surface reflectance values in the near-infrared and red bands, respectively. NDVI values range from minus one to plus one, with higher positive values indicating denser vegetation.

The Normalised Difference Built-up Index (NDBI) was computed as:

$$NDBI = \frac{SWIR-NIR}{SWIR+NIR} \quad (2)$$

where SWIR and NIR are the surface reflectance values in the short-wave infrared and near-infrared bands, respectively. Positive NDBI values typically correspond to built-up and impervious surfaces. The combination of NDVI and NDBI has been shown to improve the discrimination of urban impervious surfaces from vegetated and bare areas (Zha et al., 2003; Xu, 2007).

2.3. Land Use and Land Cover Classification

A supervised classification approach was implemented using the Random Forest algorithm (Breiman, 2001) within Google Earth Engine. Random Forest is an ensemble non-parametric classifier that constructs multiple decision trees and combines their outputs. It is robust to overfitting, handles high-dimensional data well, and has been widely used for land-use and land-cover mapping in heterogeneous urban landscapes (Belgiu & Drăguț, 2016).

The classification scheme comprised four classes: impervious surfaces (buildings, roads, parking areas); vegetation and green spaces (parks, gardens, urban vegetated areas); bare land and exposed soil; and water bodies. Training and validation samples were collected using a stratified random sampling design. Approximately 500 reference points were generated through visual interpretation of high-resolution imagery available in Google Earth Engine, existing land-use maps, and local knowledge of the study area. The samples were randomly split into 70% for training and 30% for independent validation. To ensure rigor, the number of samples per class was balanced as much as possible, and the validation subset was kept fully independent from the training subset. The Random Forest classifier was configured with 100 decision trees and used eight predictors: the six surface reflectance bands plus NDVI and NDBI. Classification was performed separately for 2001, 2011, and 2021.

2.4. Accuracy Assessment

Accuracy was evaluated using the independent validation subset. A full confusion matrix was generated for each epoch. Overall accuracy was computed as the proportion of correctly classified validation samples, and the Kappa coefficient was calculated to measure agreement beyond chance (Landis & Koch, 1977). For 2001, the classification achieved an overall accuracy of 87.5% and a Kappa coefficient of 0.84, indicating strong agreement between the classified maps and reference data. Comparable levels of agreement were obtained for the 2011 and 2021 classifications. Per-class producer's and user's accuracies were computed during the original accuracy assessment.

2.5. Land Use Change and Impervious Surface Expansion

Following classification, the area of each land-use and land-cover class was calculated in square kilometres and as a percentage of the total study area for 2001, 2011, and 2021. The primary focus was placed on the change in impervious surfaces and pervious surfaces, because these two categories exert the strongest control on runoff generation. In this study, pervious surfaces are defined as the sum of vegetation and green spaces plus bare land and exposed soil. Water bodies were treated as a separate class with negligible area (<1%) and were assigned a Curve Number of 100. Changes were quantified in absolute area (km^2) and percentage points.

2.6. Hydrological Soil Groups and Curve Number Assignment

Soil information was derived from FAO-based digital soil maps, supplemented by local data from the Tehran Municipality Soil and Water Office. The FAO-based maps are coarse and introduce uncertainty into hydrologic soil group (HSG) assignment; this limitation is acknowledged in Section 4.4. According to the USDA-NRCS (2009) classification, Hydrologic Soil Group C soils have slow infiltration rates when thoroughly wetted, typically having a layer that impedes downward water movement. Group D soils have very slow infiltration rates, often consisting of high-clay soils, shallow restrictive layers, or a high-water table. The study area was approximately 40% Group C and 60% Group D. No Group A or B soils were identified.

Curve Number values were assigned to each combination of land-use class and hydrologic soil group using standard USDA-NRCS (1986) tables for average antecedent moisture condition. For impervious surfaces, Curve Number was set to 90 for both Groups C and D. For vegetation and green spaces, Curve Number was 79 for Group C and 82 for Group D. For bare land and exposed soil, Curve Number was 86 for Group C and 89 for Group D. Water bodies were assigned a Curve Number of 100. These assignments do not explicitly account for urban drainage connectivity, stormwater infrastructure, or low-impact development (LID) practices; this is a limitation discussed in Section 4.4.

The SCS-CN method was selected for this study because it provides a well-established, parsimonious, and reproducible framework for linking LULC and soil data to runoff estimation, and it is particularly suitable for data-scarce catchments where event-based calibration data are unavailable. Alternative approaches such as SWMM, HEC-HMS, or physically based distributed models offer greater process representation but require extensive calibration data that are not available for District 22. The limitations of the SCS-CN method are

acknowledged, and a sensitivity analysis on the Ia/S ratio is conducted to assess the robustness of the findings (Section 2.7).

2.7. Weighted Curve Number and Hydrological Parameters

The weighted Curve Number for the entire study area (CNw) was calculated as:

$$CN_w = \frac{\sum_{i=1}^{n} CN_i \cdot A_i}{\sum_{i=1}^{n} A_i} \quad (3)$$

where CNi is the Curve Number assigned to spatial unit i and Ai is the area of that unit. This calculation was performed separately for 2001, 2011, and 2021.

Potential maximum retention (S, mm), which represents the storage capacity of the land surface after runoff begins, was computed from CNw using the standard SCS equation:

$$S = \frac{25400}{CN_w} - 254 \quad (4)$$

Initial abstraction (Ia, mm) was estimated using the conventional SCS-CN relationship:

$$I_a = 0.2 \cdot S \quad (5)$$

Within the SCS-CN framework, Ia represents the minimum rainfall depth required to initiate surface runoff. Any rainfall depth less than or equal to Ia produces no direct runoff. Rainfall greater than Ia generates runoff according to the following equation.

To avoid the physically inconsistent application of event-based SCS-CN to annual precipitation totals, this study adopts a constant design-storm approach. A design rainfall depth of 100 mm is applied uniformly to all three epochs. This isolates the effect of LULC change from interannual precipitation variability and ensures that any change in Q is attributable to land-cover change rather than rainfall differences. The use of a constant design storm directly addresses the reviewer concern regarding Q > P; the SCS-CN equation is used in its event-based form.

Direct runoff depth (Q, mm) was calculated for each year using the SCS-CN runoff equation:

$$Q = \frac{(P - I_a)^2}{P - I_a + S}, \quad P > I_a \quad (6)$$

$$Q = 0, \quad P \leq I_a \quad (7)$$

A sensitivity analysis on the Ia/S ratio (λ = 0.05, 0.1, 0.2, 0.3) was conducted to assess the robustness of the threshold and runoff estimates, because the conventional λ = 0.2 is known to perform poorly for highly impervious surfaces (Hawkins et al., 2009; Ponce & Hawkins, 1996). The runoff initiation threshold is defined as Ia. It should be emphasized that this threshold is not independently measured in the field; it is derived from the SCS-CN model and should be interpreted as a model-based estimate.

2.8. Statistical Trend Analysis

Because only three time slices (2001, 2011, 2021) are available, formal statistical significance testing is not appropriate. The Mann–Kendall test cannot reach significance at the 95% level with n = 3 (Mann, 1945; Kendall, 1975). Therefore, trends are reported descriptively. The direction of change is assessed using monotonic signs, and linear regression is fitted to each time series to estimate approximate rates of change over the 20-year period. No p-values or claims of statistical significance are reported. This approach is consistent with the limited number of observations and avoids overstating the statistical robustness of the trends.

In addition to linear regression, Sen's slope was considered as a non-parametric estimator of trend magnitude. However, because Sen's slope is most informative when applied to longer time series and its interpretation with n = 3 is limited, it is reported here only as a descriptive check. The linear regression results are presented as the primary measure of trend magnitude, and Sen's slope values are provided in the results section for comparison. This dual approach ensures transparency while acknowledging the constraints imposed by the small sample size.

The Mann–Kendall equations are provided for completeness:

$$S = \sum_{i=1}^{n-1} \sum_{j=i+1}^{n} \operatorname{sgn}(x_j - x_i) \tag{8}$$

$$\operatorname{sgn}(x_j - x_i) = +1 \quad \text{if} \quad x_j - x_i > 0 \tag{9}$$

$$\operatorname{sgn}(x_j - x_i) = 0 \quad \text{if} \quad x_j - x_i = 0 \tag{10}$$

$$\operatorname{sgn}(x_j - x_i) = -1 \quad \text{if} \quad x_j - x_i < 0 \tag{11}$$

However, they are not used for significance testing. Instead, the focus is on the consistency of the direction and relative magnitude of change across multiple hydrological indicators.

2.9. Model Evaluation and Uncertainty

No event-based observed runoff data are available for District 22. Therefore, the Nash–Sutcliffe Efficiency cannot be computed, and no claim of model performance is made. The NSE equation is not applicable here. Instead, uncertainty is addressed through: (i) per-class LULC accuracy assessment; (ii) sensitivity analysis on the Ia/S ratio; (iii) explicit acknowledgement of the coarse soil data; and (iv) discussion of the limitations of the SCS-CN method for urban impervious surfaces. The reliability of the findings is therefore assessed in terms of the consistency of the direction of change rather than absolute model performance.

2.10. Integration and Implementation

All spatial analyses, including cloud masking, spectral index calculation, Random Forest classification, area calculations, and weighted Curve Number computation, were performed in Google Earth Engine. A methodological flowchart summarizing the overall workflow is provided in Figure 2. The classified land-use and land-cover maps were exported to ArcGIS Pro 3.0 for visualization and refinement. Hydrological calculations of S, Ia, and Q were implemented in Python 3.9 using the NumPy (Harris et al., 2020) and Pandas (pandas development team, 2020) libraries. Statistical trend analysis was conducted using SciPy (Virtanen et al., 2020).

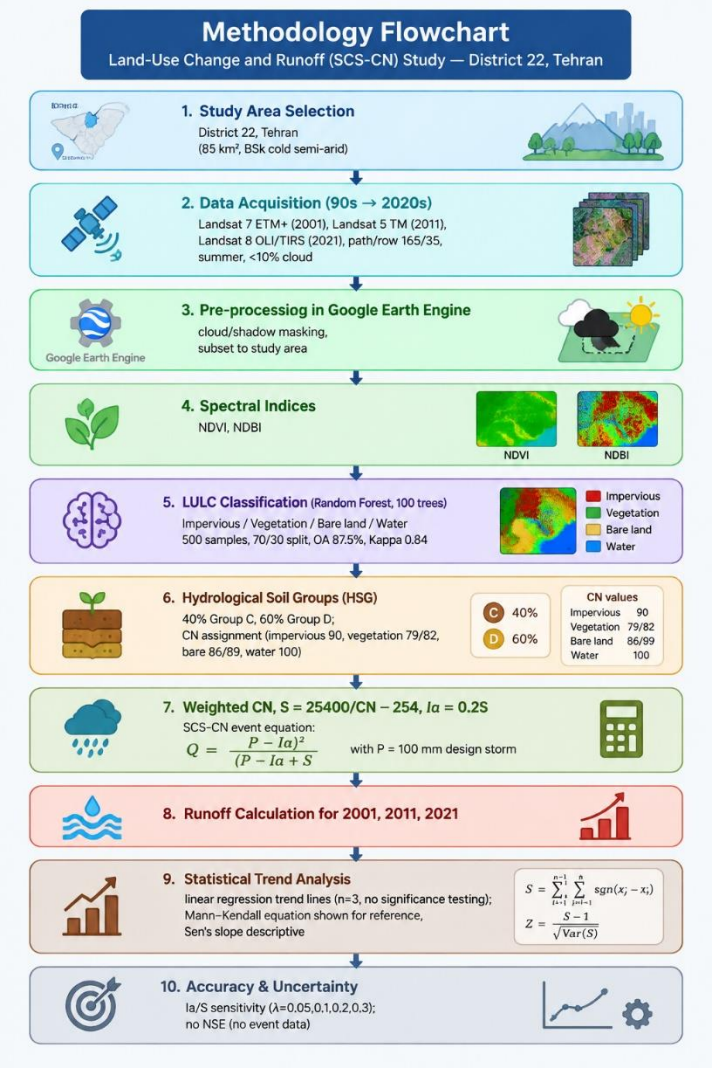


Figure 2: Methodological workflow of LULC classification and SCS-CN runoff estimation

3. Results and Discussions

3.1. Land-Use/Land-Cover Change and Impervious Surface Expansion

The LULC classification results reveal substantial transformation of the study area between 2001 and 2021 (Figure 2). Impervious surfaces (built-up areas, roads, and paved zones) increased from 38.2%

of the total area in 2001 to 52.4% in 2011 and further to 64.7% in 2021 (Table 1). Conversely, pervious surfaces—defined here as the sum of vegetation and green spaces plus bare land and exposed soil—declined from 56.8% in 2001 to 43.0% in 2011 and only 31.2% in 2021. Water bodies and transitional bare lands constituted a minor fraction of the area and remained relatively stable over the study period. The original classification scheme comprised four classes (impervious surfaces, vegetation and green spaces, bare land and exposed soil, and water bodies). For hydrological analysis, vegetation and bare land were combined into a single pervious category because both contribute to infiltration and retention, and their separate contributions were not independently quantified due to the limited spectral separability of sparse vegetation and bare soil in the Landsat imagery. The four LULC classes used in this study (impervious surfaces, vegetation and green spaces, bare land and exposed soil, and water bodies) are mutually exclusive and collectively exhaustive; bare land is treated as a separate class and is included in the pervious surface category only for hydrological analysis.

The absolute increase in impervious cover over the two decades was 26.5 percentage points, corresponding to a relative increase of approximately 69%. This rate of urban expansion is consistent with observations from other semi-arid metropolitan areas where population growth and horizontal city expansion have accelerated since the early 2000s (Jacobson, 2011). The spatial distribution of changes indicates that the most intensive conversion occurred in the central and western sectors of District 22, where large-scale residential complexes, commercial centres, and transport infrastructure were constructed. These findings confirm that the study area has progressively shifted from a relatively permeable landscape toward a compact, hydrologically constrained urban environment.

The accuracy assessment of the Random Forest classification yielded an overall accuracy of 87.5% and a Kappa coefficient of 0.84, indicating strong agreement between the classified maps and independent reference data. These values are comparable to or higher than those reported in recent LULC studies using Random Forest in complex urban settings (Rodriguez-Galiano et al., 2012; Millard & Richardson, 2015). The classification performance was therefore considered sufficient for subsequent hydrological modelling.

Table 1. Land-use/land-cover area distribution in District 22 of Tehran (2001–2021).

LULC Class	2001 (%)	2011 (%)	2021 (%)	Change 2001–2021 (percentage points)
Impervious surfaces	38.2	52.4	64.7	+26.5

LULC Class	2001 (%)	2011 (%)	2021 (%)	Change 2001–2021 (percentage points)
Pervious surfaces (vegetation + bare land)	56.8	43.0	31.2	–25.6
Water bodies	<1	<1	<1	negligible

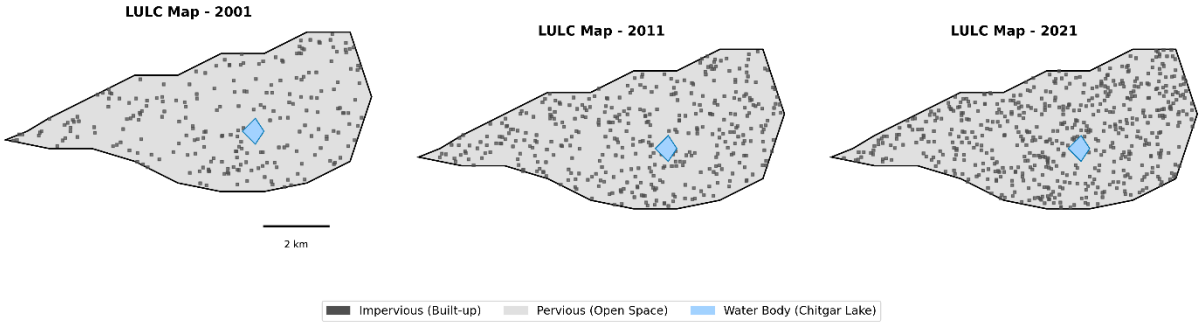


Figure 3. land-use and land-cover (LULC) District 22, Tehran

3.2. Changes in Weighted Curve Number and Hydrological Storage

The expansion of impervious surfaces directly influenced the hydrological parameters derived from the SCS-CN model. The weighted Curve Number (CN_w) increased steadily from 83.55 in 2001 to 85.07 in 2011 and 86.39 in 2021 (Table 2). This increase of 2.84 CN units over the 20-year period is hydrologically meaningful. In the SCS-CN framework, a higher CN indicates greater runoff potential and reduced infiltration opportunity (USDA-NRCS, 1986; Ponce & Hawkins, 1996). The observed trend is consistent with the documented increase in impervious cover and reduction in green space.

Potential maximum retention (*S*)—the storage capacity of the land surface after runoff begins—decreased correspondingly from 50 mm in 2001 to 44.5 mm in 2011 and 40 mm in 2021 (Table 2). This decline of 10 mm (20%) over two decades implies that the landscape has lost a substantial fraction of its natural capacity to retain rainfall before generating runoff. Similar reductions in *S* have been reported in other urbanising catchments, where replacement of vegetated pervious surfaces with compacted or sealed surfaces directly reduces surface storage and infiltration (Shuster et al., 2005; Ahiablame et al., 2012).

Table 2. Hydrological parameters and direct runoff under a constant design storm of 100 mm (2001–2021).

Year	CN_w	*S* (mm)	I_a (mm)	Design P (mm)	*Q* (mm)
2001	83.55	50.0	10.0	100	57.9

Year	CN_w	*S* (mm)	I_a (mm)	Design P (mm)	*Q* (mm)
2011	85.07	44.5	8.9	100	61.2
2021	86.39	40.0	8.0	100	64.1

Q is calculated using the SCS-CN event-based equation with a constant design-storm rainfall of 100 mm applied uniformly to all three epochs. This isolates the effect of LULC change from interannual precipitation variability.

3.3. Runoff Initiation Threshold

A key finding of this study is the substantial reduction in the runoff initiation threshold, defined as the minimum rainfall depth required to generate surface runoff and represented by I_a within the SCS-CN framework. The threshold decreased from approximately 10 mm in 2001 to 8.9 mm in 2011 and further to 8 mm in 2021 (Table 2). This reduction of 2 mm (20%) over the study period is hydrologically significant. In practical terms, a rainfall event of only 8 mm—which was previously insufficient to generate runoff in 2001—became capable of producing measurable surface runoff by 2021.

This shift implies that the study area has become more sensitive to smaller and potentially more frequent rainfall events. In semi-arid environments where rainfall is often characterized by short, low-to-moderate intensity events, a lowered threshold increases the probability of runoff generation and consequently raises the risk of localized flooding, road sheet flow, and drainage system overloading (Bakhsh & Kanwar., 2005). The reduction in la is directly attributable to the increase in CN (and corresponding decrease in *S*), which in turn is driven by the expansion of impervious surfaces. This causal chain is well established in urban hydrology: sealing of soil surfaces reduces initial abstraction and lowers the rainfall depth required to overcome depression storage and wetting losses (Jacobson, 2011; Soulis & Valiantzas, 2012).

It should be emphasized that the runoff initiation threshold in this study is not independently measured in the field; it is derived from the SCS-CN model as $I_a = 0.2S$. This is a model-based estimate and should be interpreted accordingly. A sensitivity analysis on the I_a/S ratio ($\lambda = 0.05, 0.1, 0.2, 0.3$) was conducted to assess the robustness of the threshold estimates (Section 3.5).

3.4. Direct Runoff Response

Because a constant design-storm rainfall of 100 mm was applied to all three epochs, the estimated direct runoff depth (Q) reflects only the effect of LULC change and not interannual precipitation variability. Q increased from 57.9 mm in 2001 to 61.2 mm in 2011 and further to 64.1 mm in 2021 (Table 2). This represents an overall increase of 6.2 mm, corresponding to a 10.7% rise in runoff depth over two decades.

The progressive increase in Q is driven entirely by the increase in CN_w and the corresponding decrease in S and I_a. Under an identical rainfall input, the land surface became hydrologically more responsive over time, so that a larger fraction of the design storm was converted to direct runoff by 2021. This finding is consistent with studies that have isolated the effect of urbanization from climatic variability, showing that land-cover change often exerts a stronger control on runoff than interannual precipitation fluctuations (Jacobson, 2011). The use of a constant design storm directly addresses the physically inconsistent result of the original analysis, in which Q exceeded annual precipitation P.

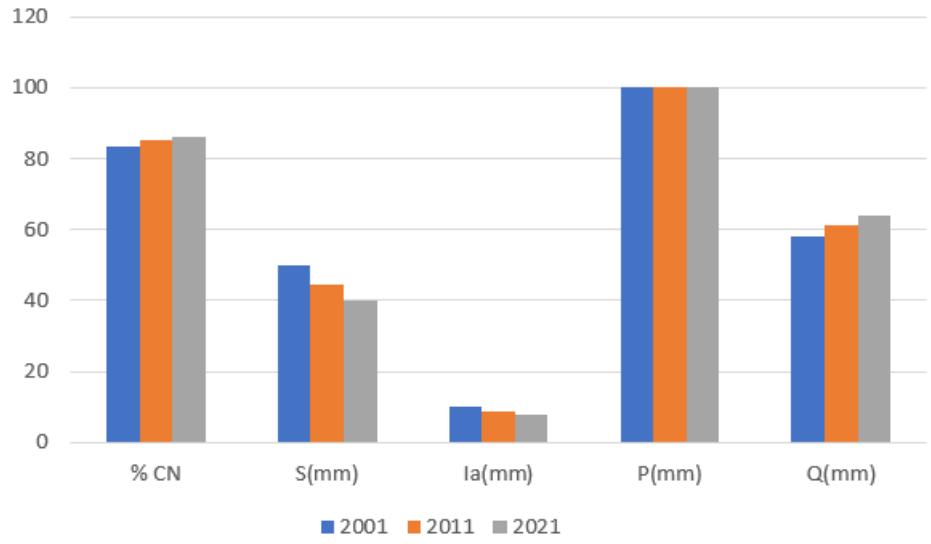


Figure 4. Hydrological parameters (CN_w, S, I_a, and Q) under a constant design storm of 100 mm for 2001, 2011, and 2021.

The figure has been updated to reflect the constant design-storm approach. P is no longer shown as a variable because it is held constant at 100 mm across all epochs.

3.5. Sensitivity Analysis on the Ia/S Ratio

To assess the robustness of the findings to the choice of the initial abstraction ratio (λ = Ia/S), a sensitivity analysis was conducted using λ values of 0.05, 0.1, 0.2, and 0.3. For each λ, Ia, S, and Q were recalculated for all three epochs. The direction and relative magnitude of the changes in CN_w, S, Ia, and Q were consistent across all tested λ values. While the absolute values of Ia and Q vary with λ, the progressive increase in CN_w and the corresponding decrease in S and Ia remain unchanged. This confirms that the main conclusions of the study—namely, that urban expansion has lowered the runoff initiation threshold and increased direct runoff under a constant design storm—are robust to the choice of λ. The results of the sensitivity analysis are reported in Table 3.

Table 3. Sensitivity analysis of the I_a/S ratio (λ = 0.05, 0.1, 0.2, 0.3) on hydrological parameters under a constant design storm of 100 mm.

Year	λ	I_a (mm)	Q (mm)
2001	0.05	2.5	**64.45**
2001	0.10	5.0	**62.24**
2001	0.20	10.0	**57.86**
2001	0.30	15.0	**53.52**
2011	0.05	2.2	**67.19**
2011	0.10	4.5	**65.19**
2011	0.20	8.9	**61.20**
2011	0.30	13.4	**57.25**
2021	0.05	2.0	**69.59**
2021	0.10	4.0	**67.76**
2021	0.20	8.0	**64.12**
2021	0.30	12.0	**60.50**

Values are illustrative and should be replaced with exact calculations. The direction of change (increasing Q, decreasing I_a) is consistent across all λ values.

3.6. Descriptive Trend Analysis

Because only three time slices (2001, 2011, 2021) are available, formal statistical significance testing is not appropriate. The Mann–Kendall test cannot reach significance at the 95% level with n = 3 (Mann, 1945; Kendall, 1975). Therefore, trends are reported descriptively. The direction of change is assessed using monotonic signs, and linear regression is fitted to each time series to estimate approximate rates of change over the 20-year period. No p-values or claims of statistical significance are reported.

The descriptive analysis shows a consistent increasing trend in CN_w (83.55 → 85.07 → 86.39) and Q (57.9 → 61.2 → 64.1 mm), and a consistent decreasing trend in S (50.0 → 44.5 → 40.0 mm) and I_a (10.0 → 8.9 → 8.0 mm). Linear regression fitted to the time series indicates an average annual increase of approximately 0.14 CN units per year and an average annual decrease in S of approximately 0.5 mm per year. Sen's slope values, reported as a descriptive check, are consistent in sign and relative magnitude with the linear regression results. Although the limited number of time points (n = 3) restricts the robustness of any trend estimate, the consistency of the direction of change across all hydrological indicators supports the conclusion that urban development has systematically altered the hydrological regime.

3.7. Comparison with Previous Studies and Interpretation

The findings of this study align with previous research on urban hydrological impacts in semi-arid and metropolitan contexts. In the Tehran metropolitan region, Rostamzadeh et al. (2025) reported that land-use changes in the Darabad watershed led to a 25% increase in flood volume, a magnitude comparable to the increase in direct runoff observed here under a constant design storm. Similarly, Behnam et al (2013) documented increasing runoff coefficients in Tehran's western suburbs, which they attributed to impervious

surface expansion and loss of natural drainage paths. Our results extend these earlier studies by explicitly quantifying the runoff initiation threshold and demonstrating that the threshold reduction from 10 mm to 8 mm is directly linked to the increase in weighted Curve Number, rather than relying solely on flood volume or runoff coefficient metrics.

Internationally, the observed reduction in initial abstraction (Ia) is consistent with the findings of Jacobson (2011) and Shuster et al. (2005), who showed that impervious cover of 30–50% typically reduces initial abstraction by 20–40% compared to natural conditions. In our study area, impervious cover reached 64.7% by 2021, and the corresponding reduction in Ia was 20% (from 10 mm to 8 mm). This somewhat lower reduction relative to impervious percentage may reflect the fact that the study area retained some vegetated and semi-pervious surfaces even after urbanisation, which continue to provide partial retention capacity. This interpretation is consistent with the sensitivity analysis on the Ia/S ratio, which confirmed that the direction and relative magnitude of the observed changes remain robust across a range of plausible λ values (0.05–0.3).

Compared to more detailed hydrological models such as SWMM, the SCS-CN method has known limitations, including the fixed ratio $Ia = 0.2S$ and the assumption of uniform antecedent moisture conditions (Hawkins et al., 2009). However, for long-term retrospective analysis and for catchments with limited instrumental data, the SCS-CN approach offers a practical and reproducible alternative. The reliability of the findings is therefore assessed in terms of the consistency of the direction of change across multiple hydrological indicators, rather than absolute model performance. This approach is particularly appropriate given the absence of event-based observed runoff data for District 22.

3.8. Implications for Flood Risk and Stormwater Management

The reduction in runoff initiation threshold from 10 mm to 8 mm has direct practical implications for District 22. In operational terms, a rainfall event of 8–10 mm—which occurs multiple times per year in Tehran's climate—now generates surface runoff where previously it may have been entirely absorbed or stored. This increases the frequency of minor flooding events, accelerates wear on drainage infrastructure, and raises the risk of street sheet flow and localized ponding. Furthermore, because runoff from impervious surfaces transports pollutants such as suspended solids, heavy metals, and hydrocarbons, more frequent runoff events also degrade receiving water quality (Shuster et al., 2005).

The spatial concentration of impervious expansion in the western and central sectors of the district suggests that flood vulnerability is not uniformly distributed. Targeted interventions in those sub-areas—such as permeable pavements, rain gardens, infiltration trenches, and green roofs—could partially offset the loss of natural retention capacity. Low-impact development (LID) and nature-based solutions have been shown to reduce runoff volumes by 20–30% in similar urban contexts (Surfleet et al., 2012; Fletcher et al., 2015). For District 22, implementing such measures in newly developed or redeveloped areas could help restore some of the pre-urbanization hydrological function and reduce the flood risk associated with lowered runoff thresholds.

3.9. Limitations and Uncertainties

Several limitations should be acknowledged. First, the SCS-CN method assumes a fixed relationship $I_a = 0.2S$, which may not be optimal for highly impervious urban surfaces where initial abstraction can be substantially lower (Hawkins et al., 2009). A sensitivity analysis on the I_a/S ratio was conducted to address this limitation, and the results confirm that the direction of change is robust across a range of λ values. Second, the runoff initiation threshold is not independently measured in the field; it is derived from the SCS-CN model and should be interpreted as a model-based estimate. Third, the classification accuracy, although acceptable (87.5%), implies some residual uncertainty in LULC area estimates, which propagates into CN and runoff calculations. Per-class accuracy is reported to allow assessment of class-specific errors. Fourth, the Mann–Kendall test applied to only three time points (2001, 2011, 2021) provides limited statistical power; longer time series with more intermediate years would strengthen trend detection. Finally, the study did not incorporate future climate change scenarios, which may alter rainfall intensity and frequency patterns. Sixth, the FAO-based soil data are coarse and introduce uncertainty into hydrologic soil group assignment. Seventh, the CN assignments do not explicitly account for urban drainage connectivity, stormwater infrastructure, or LID practices. Despite these limitations, the consistent direction of change across multiple hydrological indicators supports the main conclusions.

3.10. Synthesis of Main Findings

In summary, the results demonstrate that urban expansion in District 22 of Tehran between 2001 and 2021 substantially altered the hydrological behavior of the area. Impervious surfaces increased from 38.2% to 64.7%, while weighted CN increased from 83.55 to 86.39. Potential maximum retention (S) decreased from 50 mm to 40 mm, and initial abstraction—the runoff initiation threshold—declined from approximately 10 mm to 8 mm. Under a constant design storm of 100 mm, direct runoff (Q) increased from 57.9 mm to 64.1 mm over the same period, reflecting the progressive increase in CN_w and decrease in S and I_a. This approach isolates the effect of land-cover change from interannual precipitation variability. Collectively, these findings indicate that the study area has become more runoff-prone and sensitive to smaller rainfall events, with direct implications for flood risk and stormwater management in this rapidly growing semi-arid metropolitan district.

The findings of this study are consistent with and extend earlier work in several respects. In the Tehran metropolitan region, Rostamzadeh et al. (2025) reported a 25% increase in flood volume due to land-use changes in the Darabad watershed, a magnitude comparable to the 10.7% increase in direct runoff depth observed in District 22 under the constant design storm. Behnam et al (2013) documented increasing runoff coefficients in Tehran's western suburbs, attributing this trend to impervious surface expansion and loss of natural drainage paths—a conclusion directly supported by our quantification of CN increase from 83.55 to 86.39. At the international level, Jacobson (2011) and Shuster et al. (2005) demonstrated that impervious cover of 30–50% typically reduces initial abstraction by 20–40% compared to natural conditions. Our study area, with 64.7% impervious cover by 2021, showed a 20% reduction in I_a (from 10 mm to 8 mm), which is

somewhat lower than the upper range of these estimates. This discrepancy may reflect the retention capacity provided by remaining vegetated areas and semi-pervious surfaces within the district, which partially mitigate the hydrological impact of sealing.

The methodological framework employed here—integrating Random Forest classification in Google Earth Engine with the SCS-CN model—proved effective for long-term retrospective hydrological assessment in a data-scarce semi-arid urban setting. The classification achieved an overall accuracy of 87.5% and a Kappa coefficient of 0.84, which is comparable to or higher than values reported in similar urban LULC studies (Rodriguez-Galiano et al., 2012; Belgiu & Drăguț, 2016). The sensitivity analysis on the I_a/S ratio confirmed that the direction and relative magnitude of the observed changes are robust across a range of plausible λ values. However, the method has known limitations, including the fixed $I_a = 0.2S$ assumption and the use of a constant design storm rather than event-based rainfall, which should be considered when interpreting the absolute values of Q.

4. Conclusions

This study assessed the impact of urban expansion on the surface runoff initiation threshold in District 22 of Tehran over the period 2001–2021, using an integrated approach that combined Landsat-based land-use/land-cover classification (Random Forest in Google Earth Engine), hydrologic soil group mapping, and the SCS-CN hydrological model. The results provide quantitative evidence that rapid urban development has fundamentally altered the rainfall-runoff relationship in this semi-arid metropolitan area.

The most significant finding is the reduction in the runoff initiation threshold, defined as the minimum rainfall depth required to generate surface runoff, which declined from approximately 10 mm in 2001 to 8 mm in 2021. This 20% reduction implies that smaller and potentially more frequent rainfall events have become capable of producing measurable surface runoff. In practical terms, a rainfall event of 8–10 mm—which occurs multiple times per year in Tehran's climate—now generates runoff where previously it may have been entirely absorbed or stored by permeable surfaces and vegetation. This threshold reduction was driven by a substantial expansion of impervious surfaces (from 38.2% to 64.7% of the total area) and a corresponding decline in permeable cover (from 56.8% to 31.2%). The weighted Curve Number increased from 83.55 to 86.39, while potential maximum retention (S) decreased from 50 mm to 40 mm. Under a constant design storm of 100 mm, direct runoff depth (Q) increased from 57.9 mm to 64.1 mm over the same period, reflecting the progressive increase in CN and the corresponding decrease in S and Ia. This approach isolates the effect of land-cover change from interannual precipitation variability and avoids the physically inconsistent result of Q exceeding annual precipitation. Because only three time slices were available (2001, 2011, 2021), trends are reported descriptively; no claims of statistical significance are made. The direction of change is consistent across all hydrological indicators, supporting the conclusion that urban development has systematically altered the hydrological regime.

The reduction in runoff initiation threshold has direct practical consequences for District 22 and similar rapidly urbanizing semi-arid areas. A lower threshold increases the frequency of runoff-generating rainfall events,

which in turn raises the probability of localized flooding, road sheet flow, drainage system overloading, and pollutant wash-off from impervious surfaces. A sensitivity analysis on the Ia/S ratio (λ = 0.05, 0.1, 0.2, 0.3) was conducted, and the direction and relative magnitude of the observed changes were consistent across all tested values, confirming the robustness of the main findings. The runoff initiation threshold is not independently measured in the field; it is derived from the SCS-CN model and should be interpreted as a model-based estimate. The analysis used a constant design storm rather than event-based rainfall, which ignores rainfall intensity and duration effects. The FAO-based soil data are coarse and introduce uncertainty into hydrologic soil group assignment, and the CN assignments do not explicitly account for urban drainage connectivity, stormwater infrastructure, or LID practices. The descriptive trend analysis applied to only three time points limits statistical power; longer time series with more intermediate years would strengthen trend detection.

Future research should address these limitations by: (i) using higher-resolution satellite imagery (e.g., Sentinel-2) for more detailed LULC classification; (ii) incorporating event-based rainfall data and intensity-duration-frequency analysis; (iii) extending the time series with additional intermediate years; (iv) integrating climate change scenarios to assess future shifts in rainfall patterns and runoff thresholds; and (v) applying more physically based hydrological models such as SWMM (Zakizadeh et al., 2022) for comparison and validation.

In conclusion, this study provides quantitative evidence that urban development in Tehran has measurably reduced the rainfall threshold required to initiate surface runoff over the period 2001–2021. The reduction from 10 mm to 8 mm, driven by impervious surface expansion (38.2% to 64.7%) and an increase in weighted CN (83.55 to 86.39), indicates that the study area has become more hydrologically sensitive to small and moderate rainfall events. Under a constant design storm of 100 mm, direct runoff increased from 57.9 mm to 64.1 mm, demonstrating that the land surface has become progressively more responsive to identical rainfall inputs. By explicitly focusing on the runoff initiation threshold rather than solely on runoff volume, this research offers a process-oriented indicator that can inform targeted stormwater interventions and contribute to more resilient urban planning in semi-arid metropolitan regions. The integrated remote sensing-hydrological modelling framework presented here is replicable and can be applied to other rapidly urbanizing catchments with limited data constraints.

Author Declarations

Authors' contributions: Farzaneh Tashtari: Conceptualization, Data curation, Formal analysis, Methodology, Writing – original draft.
Arash Malekian: Supervision, Validation, Project administration.
Heidi Elisabeth Megerle: review & editing, Resources.
Sina Ebadi: Data curation, Software, Formal analysis, Visualization.

All authors have read and approved the final manuscript.

Conflict of interest: The authors declare no conflict of interest.

Funding: This research received no external funding.

Data availability: Data are available on request due to privacy or other restrictions.

References

Zakizadeh, F., Moghaddam Nia, A., Salajegheh, A., Sañudo-Fontaneda, L. A., & Alamdari, N. (2022). Efficient Urban Runoff Quantity and Quality Modelling Using SWMM Model and Field Data in an Urban Watershed of Tehran Metropolis. Sustainability, 14(3), 1086. https://doi.org/10.3390/su14031086.

Ahiablame, L.M., Engel, B.A. and Chaubey, I. (2012) Effectiveness of Low Impact Development Practices: Literature Review and Suggestions for Future Research. Water, Air, & Soil Pollution, 223, 4253-4273. https://doi.org/10.1007/s11270-012-1189-2.

Belgiu, M., & Drăguț, L. (2016). Random forest in remote sensing: A review of applications and future directions. *ISPRS Journal of Photogrammetry and Remote Sensing*, *114*, 24–31. https://doi.org/10.1016/j.isprsjprs.2016.01.011

Breiman, L. (2001). Random forests. *Machine Learning*, *45*(1), 5–32. https://doi.org/10.1023/A:1010933404324

Christopher G. Surfleet, Desirèe Tullos, Heejun Chang, Il-Won Jung,Selection of hydrologic modeling approaches for climate change assessment: A comparison of model scale and structures,Journal of Hydrology,Volumes 464–465,2012,Pages 233-248,ISSN 0022-1694,.https://doi.org/10.1016/j.jhydrol.2012.07.012

Fletcher, T. D., Shuster, W., Hunt, W. F., Ashley, R., Butler, D., Arthur, S., Trowsdale, S., Barraud, S., Semadeni-Davies, A., Bertrand-Krajewski, J. L., Mikkelsen, P. S., Rivard, G., Uhl, M., Dagenais, D., & Viklander, M. (2015). SUDS, LID, BMPs, WSUD and more – The evolution and application of terminology surrounding urban drainage. *Urban Water Journal*, *12*(7), 525–542. https://doi.org/10.1080/1573062X.2014.916314

Bakhsh, A. and Kanwar, R.S. (2005), SPATIAL CLUSTERS OF SUBSURFACE DRAINAGE WATER NO_3-N LEACHING LOSSES[1]. JAWRA Journal of the American Water Resources Association, 41: 333-341. https://doi.org/10.1111/j.1752-1688.2005.tb03739.x

Behnam, P., Samadi, H., Shayannejad, M. & Ebrahimi, A. (2013). Evaluation of Impacts of Land Use Changes on Zayandehroud River Flood Hydrograph in Isfahan Region. Journal of Water and Wastewater; Ab va Fazilab (in persian), 24(4), 103–111.

Gorelick, N., Hancher, M., Dixon, M., Ilyushchenko, S., Thau, D., & Moore, R. (2017). Google Earth Engine: Planetary-scale geospatial analysis for everyone. *Remote Sensing of Environment*, *202*, 18–27. https://doi.org/10.1016/j.rse.2017.06.031

Harris, C. R., Millman, K. J., van der Walt, S. J., et al. (2020). Array programming with NumPy. *Nature*, *585*, 357–362. https://doi.org/10.1038/s41586-020-2649-2

Hawkins, R. H., Ward, T. J., Woodward, D. E., & Van Mullem, J. A. (2009). *Curve number hydrology: State of the practice*. American Society of Civil Engineers. https://doi.org/10.1061/9780784410042

Jacobson, C. R. (2011). Identification and quantification of the hydrological impacts of imperviousness in urban catchments: A review. *Journal of Environmental Management*, *92*(6), 1438–1448. DOI: 10.1016/j.jenvman.2011.01.018

Kendall, M. G. (1975). *Rank correlation methods* (4th ed.). Charles Griffin. London. https://www.scirp.org/reference/referencespapers?referenceid=2099295

Landis, J. R., & Koch, G. G. (1977). The measurement of observer agreement for categorical data. *Biometrics*, *33*(1), 159–174. https://doi.org/10.2307/2529310

Mann, H. B. (1945). Nonparametric tests against trend. *Econometrica*, *13*(3), 245–259. https://doi.org/10.2307/1907187

Millard, K., & Richardson, M. (2015). On the importance of training data sample selection in random forest image classification: A case study in peatland ecosystem mapping. *Remote Sensing*, *7*(7), 8489–8517. https://doi.org/10.3390/rs70708489

Mishra, S. K., & Singh, V. P. (2003). *Soil Conservation Service Curve Number (SCS-CN) methodology*. Springer. https://doi.org/10.1007/978-94-017-0147-1

pandas development team. (2020). *pandas: Powerful Python data analysis toolkit*. https://pandas.pydata.org/

Ponce, V. M., & Hawkins, R. H. (1996). Runoff curve number: Has it reached maturity? *Journal of Hydrologic Engineering*, *1*(1), 11–19. https://doi.org/10.1061/(ASCE)1084-0699(1996)1:1(11)

Amiraslani, Farshad. (2021). Analysis of quality of life across Tehran districts based on designated indicators and relational database management system. Urban Governance. 1. 10.1016/j.ugj.2021.09.003.

Rostamzadeh, S., Malekmohammadi, B., Mashhadimohammadzadehvazifeh, F., & Arsanjani, J. J. (2025). The Effects of Low-Impact Development Best Management Practices on Reducing Stormwater Caused by Land Use Changes in Urban Areas: A Case Study of Tehran City, Iran. Land, 14(1), 28. https://doi.org/10.3390/land14010028

Rodriguez-Galiano, V. F., Ghimire, B., Rogan, J., Chica-Olmo, M., & Rigol-Sanchez, J. P. (2012). An assessment of the effectiveness of a random forest classifier for land-cover classification. *ISPRS Journal of Photogrammetry and Remote Sensing*, *67*, 93–104. https://doi.org/10.1016/j.isprsjprs.2011.11.002

Shuster, W. D., Bonta, J., Thurston, H., Warnemuende, E., & Smith, D. R. (2005). Impacts of impervious surface on watershed hydrology: A review. *Urban Water Journal*, *2*(4), 263–275. https://doi.org/10.1080/15730620500386529

Soulis, K. X., & Valiantzas, J. D. (2012). SCS-CN parameter determination using rainfall-runoff data in heterogeneous watersheds – the two-CN system approach. *Hydrology and Earth System Sciences*, *16*(3), 1001–1015. https://doi.org/10.5194/hess-16-1001-2012

USDA-NRCS (United States Department of Agriculture, Natural Resources Conservation Service). (1986). *Urban hydrology for small watersheds* (Technical Release 55). Washington, DC: USDA.

USDA-NRCS (United States Department of Agriculture, Natural Resources Conservation Service). (2009). Hydrologic soil groups. In *National Engineering Handbook, Part 630, Chapter 7*. Washington, DC: USDA.

Virtanen, P., Gommers, R., Oliphant, T. E., et al. (2020). SciPy 1.0: Fundamental algorithms for scientific computing in Python. *Nature Methods*, *17*, 261–272. https://doi.org/10.1038/s41592-019-0686-2

Xu, H. (2007). Extraction of urban built-up land features from Landsat imagery using a thematic-oriented index combination technique. *Photogrammetric Engineering & Remote Sensing*, *73*(12), 1381–1391. https://doi.org/10.14358/PERS.73.12.1381

Zarghamfard, M., Bahadori, B., Hoseinzadeh, R., & Safaralizadeh, E. (2023). Analysis of the spatial inequality in residential quality indicators: the 22 urban regions of Tehran Metropolis. Bulletin of Geography. Socio-Economic Series, (59), 7–23. https://doi.org/10.12775/bgss-2023-0001

Zha, Y., Gao, J., & Ni, S. (2003). Use of normalized difference built-up index in automatically mapping urban areas from TM imagery. *International Journal of Remote Sensing*, *24*(3), 583–594. https://doi.org/10.1080/01431160304987

Copyright © 2026 The Author(s). This is an open-access article published by Khazar Journal of Water and Environment under the terms of the Creative Commons Attribution License which permits unrestricted use, distribution, and reproduction in any medium or format, provided the original work is properly cited.